

Universal set of Observables for Forecasting Physical Systems through Causal Embedding

G Manjunath*, A de Clercq* & MJ Steynberg†

*Department of Mathematics & Applied Mathematics, † Department of Physics, University of Pretoria, Pretoria 0028

Email: manjunath.gandhi@up.ac.za ; decle029@umn.edu ; thys.steynberg@tuks.co.za

Abstract

We demonstrate when and how an entire left-infinite orbit of an underlying dynamical system or observations from such left-infinite orbits can be uniquely represented by a pair of elements in a different space, a phenomenon which we call *causal embedding*. The collection of such pairs is derived from a driven dynamical system and is used to learn a function which together with the driven system would: (i). determine a system that is topologically conjugate to the underlying system (ii). enable forecasting the underlying system's dynamics since the conjugacy is computable and universal, i.e., it does not depend on the underlying system (iii). guarantee an attractor containing the image of the causally embedded object even if there is an error made in learning the function. By accomplishing these we herald a new forecasting scheme that beats the existing reservoir computing schemes that often lead to poor long-term consistency as there is no guarantee of the existence of a learnable function, and overcomes the challenges of stability in Takens delay embedding. We illustrate accurate modeling of underlying systems where previously known techniques have failed.

Introduction. Performing experimental measurements on physical, biological and artificial deterministic systems to obtain a more informative dynamical model with applications in better control and management of resources and service interruptions has been well established in modern-day science. Attempts to build models from complex data such as sunspot cycles date back to the 1920s in [1]. Although our ability to collect data has vastly improved ever since, and data-driven machine learning methods have gained popularity, the quest for the right observables, like the delay-coordinates in Takens delay embedding [2] along with stability in forecasting has remained elusive.

The Takens delay embedding theorem and its generalizations (e.g., [3, 4, 5]) essentially guarantee that when observations $(\theta(w_i), \theta(w_{i+1}), \dots)$ of an orbit (w_i, w_{i+1}, \dots) of an unknown invertible dynamical system $S : W \rightarrow W$, where W is a space whose dimension can be well-defined (like a manifold) and has dimension d , the functions S , and $\theta : W \rightarrow \mathbb{R}$ belong to a generic class of smooth functions, and $w_{n+1} = S(w_n)$ for each w_n in W and integer n , then the delay coordinates $\Phi_{2d,\theta} : W \rightarrow \mathbb{R}^{2d+1}$ given by $\Phi_{2d,\theta}(w) := (\theta(S^{-2d}w), \dots, \theta(S^{-1}w), \theta(w))$ is an embedding of W in \mathbb{R}^{2d+1} (i.e. $\Phi_{2d,\theta} : \Phi_{2d,\theta}(W) \rightarrow \Phi_{2d,\theta}(W)$ is a homeomorphism). Consequently, there exists a function/map between the delay coordinates $F_S : (\theta(S^{-2d}(w)), \dots, \theta(S^{-1}(w)), \theta(w)) \mapsto (\theta(S^{-2d+1}(w)), \dots, \theta(w), \theta(S(w)))$. Hence, by observing successive data points in the space of delay coordinates, one can learn the map F_S which then leads to forecasting of the observations obtained from θ . The salient feature of Takens delay embedding is that the delay coordinate map by $\Phi_{2d,\theta}$ is a universal observable of the data, i.e., for a fixed delay d , it does not change (but only adjusts its domain) even if the underlying W , S or θ are changed. Next, Takens' result makes $\Phi_{2d,\theta}$ a conjugacy (we refer to [6] for basic terminologies) that results in $F_S \circ \Phi_{2d,\theta} = \Phi_{2d,\theta} \circ S$ (or the diagram in Fig 1C in green commutes). Since the conjugacy establishes a one-to-one correspondence between the orbits of S and F_S , a model F_S is particularly helpful in understanding the global behavior of S when long-term pointwise prediction is not possible, for instance, when S exhibits sensitive dependence on initial conditions.

The above results all hold when a delay-coordinate map $\Phi_{K,\theta}$ is used when $K \geq 2d+1$. In practice, iterating F_S in the presence of errors can amplify the error depending on θ and K used (see [7] for a detailed discussion). In particular, we note the delay-coordinates can take values outside the embedded set $\Phi_{2d,\theta}(W)$ (see Fig. 1A), and hence \tilde{F}_S , an extension [8] of the map F_S that is defined on a neighborhood of $\Phi_{2d,\theta}(W)$ is used to generate the dynamics in practice (e.g., by a feedforward neural network). While doing so, the F_S -embedded object $\Phi_{2d,\theta}(W)$ cannot be expected to be an attractor of an extension \tilde{F}_S since the extension \tilde{F}_S behaves much like F_S in a neighborhood of $\Phi_{2d,\theta}(W)$. Thus \tilde{F}_S can be locally expanding in a neighborhood of $\Phi_{2d,\theta}(W)$. Hence for an x lying outside $\Phi_{2d,\theta}(W)$, its future iterates could be veering far off from $\Phi_{2d,\theta}(W)$ thereby leading to miscarried forecasting/ modeling.

Global approximation strategies that discover a single data-fitting function F_S frequently perform well, but often only if it has a low-functional complexity, which is a subjective measure of “wiggleness” of the graph of a function (see discussion in [9]). Takens along with his co-authors in [10] allude to this issue when neural networks used for learning F_S often fail (also see [11]).

Recent Koopman operator-based data-driven methods use non-standardized observable selection (e.g., [12, 13]). Library-based methods [14, 15, 16] that require the vector field or a map to lie in the span of a pre-determined set of basis functions give interpretable models but require complete knowledge of the underlying state space

variables and data with higher sampling rates, which is rare in practice.

Existing machine learning following reservoir computing techniques [17, 18] are more noise-resistant, have simpler training methods, and often choose to learn a “linear” map with low functional complexity, even though the existence of a learnable map that can precisely predict the dynamics is unknown. A lack of learnability results in poor long-term consistency [19, 20, 21] – such systems employed are listed later here. This learnability problem is solved by a generic linear driven system in [22], but the learnt system can suffer the same stability problem while as in learning F_S above.

We intend to overcome these challenges by obtaining the best of the above methods in the sense that we can embed W in a new space using observations when Takens embedding holds for the delay coordinates so that $f(W)$ is contained in an attractor of its extension. This allows noisy trajectories to be “stabilized” back as in Fig. 1B instead of veering off as indicated in Fig. 1A and provides remarkable robustness to noise.

To define such an embedding f , we consider the recursive dynamics of a continuous map $g : U \times X \rightarrow X$. Here, we assume U and X to be nonempty compact metric spaces. We call a function g , a driven system with the input space U and its “state space” X quietly understood. A bi-infinite sequence $\{x_n\}$ is called a solution of g for an input $\{u_n\}$ if $x_{n+1} = g(u_n, x_n)$ holds for all $n \in \mathbb{Z}$. Driven systems have at least one solution for a given input (e.g., [23]). A particularly interesting case: if for each input $\bar{u} = \{u_n\}$ there exists exactly one solution, we say that g has the unique solution property (USP) i.e., there is a well-defined solution map $\Psi : \bar{u} \mapsto \{x_n\}$. In the field of reservoir computing, $\Psi(\bar{u})$ is meant to act as a proxy of the input sequence \bar{u} , but we warn the reader that Ψ is not necessarily injective when g has the USP (example in [9]) but can be made so with the SI-invertibility condition defined below. The USP is equivalent to the echo state property [23] in the vast reservoir computing literature inspired by [17, 24], and is an asymptotic state contraction property that has been well-studied [25, 26]. A remarkable feature of a driven system with the USP is that the “future states” of a solution need not be solved analytically, but can be computed iteratively without the need for the entire-left infinite history of the input thanks to the “uniform attraction property” (UAP) [27, 9]. Precisely, given any input \bar{u} and its solution $\Psi(\bar{u})$, for every $\epsilon > 0$, by initializing the driven system with an arbitrary initial value $y_m \in X$, then the “state-trajectory” y_{m+1}, y_{m+2}, \dots satisfying $y_{j+1} = g(u_j, y_j)$ for $j \geq m$ is such that the distance between x_{m+i} and y_{m+i} is less than ϵ for all $i \geq k$ where (importantly) k can be chosen independently of both y_m and the input \bar{u} (see [27, Theorem 1] or [9]).

A dynamical system in this work is a tuple (U, T) where U is a compact metric space and $T : U \rightarrow U$ is a surjective function (that is not necessarily continuous). When

T is not surjective to start with we can restrict the non-transient dynamics to an invariant set A (i.e., $T(A) := \cup_{u \in A} T(u) = A$) and T restricted to A is surjective. Due to the surjectivity, We call a bi-infinite sequence $\bar{u} = \{u_n\}_{n \in \mathbb{Z}}$ that obeys the update equation, $u_{n+1} = T(u_n)$ where $n \in \mathbb{Z}$ as an orbit/trajectory of T , and since T is surjective there is at least one orbit “through” each point in U .

Finding an equivalent dynamical system to (U, T) means finding another dynamical system (U', T') so that there exists a homeomorphism $\phi : U \rightarrow U'$ with the property that $\phi \circ T = T' \circ \phi$. Such a map ϕ is called a conjugacy and we say that (U', T') is conjugate to (U, T) or simply T' is conjugate to T . If we relax the condition on ϕ where, instead of having a homeomorphism, we only require ϕ to be continuous, then we call ϕ a semi-conjugacy, and say that T' is semi-conjugate to T . When T' is semi-conjugate to T then it is customary to say that T is a (dynamical) extension of T' and captures the dynamics of T , while T' cannot have any additional complexity (measured through topological entropy) than present in T (e.g., [6]). Our aim here is to build a model that is either conjugate or a (dynamical) extension of the underlying system so that the underlying system can be forecasted.

Driven systems have an analog of semi-conjugacy too [27]. For learning the underlying input dynamics using a driven system, its solution should not have additional “complexity” (see [9]) than that is present in the input. Hence there needs to be a function called the universal semi-conjugacy h mapping a left-infinite sequence in U to X so that $h \circ \sigma_v = g(v, \cdot) \circ h$ where $\sigma_v((\dots, u_{-2}, u_{-1})) = (\dots, u_{-2}, u_{-1}, v)$ [27] (equivalently the diagram in [9] commutes).

When the inputs to g are restricted to be orbits of (U, T) the states of the system at any time instant n can be considered to depend on the left-infinite history of the input $(\dots, u_{n-2}, u_{n-1})$, i.e, on a left-infinite orbit of T . The space of left-infinite orbits

$$\widehat{U}_T := \{(\dots, u_{-2}, u_{-1}) : Tu_n = u_{n+1}\},$$

is called the inverse-limit space of (U, T) (e.g., [28]); in the literature, the elements of \widehat{U}_T are customarily written as right-infinite sequences. The map T also induces a self-map \widehat{T} on \widehat{U}_T defined by $\widehat{T} : (\dots, u_{-2}, u_{-1}) \mapsto (\dots, u_{-2}, u_{-1}, T(u_{-1}))$. It is straightforward to observe that $\varphi_T : U \rightarrow \widehat{U}_T$, $\varphi_T : u \mapsto (\dots, T^{-2}(u), T^{-1}(u), u)$ is a conjugacy between T and \widehat{T} i.e., the diagram (in Fig. 1C printed in yellow-blue) commutes.

We say a driven system g *causally embeds* a dynamical system (U, T) if it satisfies the two properties: (i) a universal semi-conjugacy h exists and (ii) a function $H_2 : \widehat{U}_T \rightarrow X \times X$, defined by $H_2((\dots, u_{-2}, u_{-1})) := (h((\dots, u_{-3}, u_{-2})), h((\dots, u_{-2}, u_{-1})))$ embeds the inverse-limit space \widehat{U}_T in $X \times X$, i.e., there exists a set $Y_T \subset X \times X$ so that $H_2 : \widehat{U}_T \rightarrow Y_T$ is a homeomorphism. The remarkable feature is that the ability

of a driven system to causally embed a dynamical system does not depend on the map T on U since H_2 is purely determined by g , and so the domain of H_2 defined above through h can be likewise extended to the space of left-infinite sequences contained in U – from a practical viewpoint, this means that if the self-map T is changed to another \mathfrak{T} on U , the driven system g does not need to change and when H_2 is considered or restricted to be defined only on $\widehat{U}_{\mathfrak{T}}$, it still embeds $\widehat{U}_{\mathfrak{T}}$ in $X \times X$. Hence, H_2 acts as a universal $X \times X$ -valued observable for any dynamical system on U just like the delay-coordinate map $\Phi_{2d,\theta}$ is a universal observable that does not depend on the map S on W . Our interest in this universal observable is due to the map h (and thus H_2 here) that can also be a differentiable conjugacy since h inherits the smoothness properties from g [29], and if g_λ is continuous in the parameter λ , so would the conjugacy.

Now, here are sufficient conditions on g under which it can causally embed (U, T) (we present a formal proof in [9]) when T is a homeomorphism: (a) g has the USP and (b) g satisfies the state-input (SI) invertibility condition, i.e. $g(\cdot, x) : U \rightarrow X$ is invertible for all x (or in other words if $x_{n+1} = g(u_n, x_n)$ then (x_{n+1}, x_n) uniquely determines u_n).

An example of g . We consider a recurrent neural network (RNN), a driven system with both $U, X \subset \mathbb{R}^N$ that is defined through

$$x_{n+1} = (1 - a)x_n + a\overline{\tanh}(Au_n + \alpha Bx_n), \quad (1)$$

where A and B are real invertible matrices of dimension $N \times N$ and $\overline{\tanh}(\ast)$ is the \tanh performed component-wise on \ast , and $0 < \alpha$, $0 < a \leq 1$ are reals; a sufficient condition for g to have the USP is that the norm of αB is less than 1 (see [30]). It suffices that when we allow A and B to be invertible, u_n can be recovered given (x_n, x_{n+1}) (see [9]).

Exploitation of Causal Embedding. In the customary RC approach [31, 18], an RNN of the type (1) is used where a matrix A has a dimension $N \times K$ where $K < N$ and the observations $\{\theta(w_n)\}$ (where $w_{n+1} = S(w_n)$ and $\theta : W \rightarrow [-1, 1]$) is fed into the RNN sequentially. Here, we assume that Takens delay embedding holds or in other words $\Phi_{2d,\theta}$ embeds W in \mathbb{R}^{2d+1} (or the commutativity shown in green in Fig. 1C holds). We then pad adequate zeroes to the delay-coordinates before feeding it sequentially into the RNN (as an orbit of T described below). Precisely, we take $U = [-1, 1]^N$ where $N > K \geq 2d + 1$, and $(U, T) := (P(\Phi_{2d,\theta}(W)), F'_S)$, where $P : \Phi_{2d,\theta}(W) \rightarrow U$ is defined as $P : v_n \mapsto (v_n^1, v_n^2, \dots, v_n^K, 0, 0, \dots, 0)$ and $F'_S = P \circ \Phi_{2d,\theta} \circ F_S \circ \Phi_{2d,\theta}^{-1} \circ P^{-1}$ is a self-map on $\Phi_{2d,\theta}(W)$. This entails F'_S to be conjugate to S , i.e., the diagram in Fig. 1C (printed in green-yellow) commutes. Now, if the RNN g can causally embed (U, T) , the self-map $G_T : H_2 \circ \widehat{T} \circ H_2^{-1}$ on Y_T is well-defined, and G_T is conjugate to \widehat{T} and hence to T as seen in the commutativity ladder in Fig 1C. Thus from this commutativity ladder G_T is conjugate to S and

$f = H_2 \circ \varphi_T \circ P \circ \Phi_{2d,\theta}$ is the conjugacy between (W, S) and (Y_T, G_T) or embeds W in $X \times X$.

To conceive the causal embedding, we assume g to be SI-invertible in which case a “read-out” function $\Gamma : Y_T \rightarrow U$ that is defined by $\Gamma : (x_{j-1}, x_j) \mapsto u_j$ exists (see [9]) where $\{x_k\} = \Psi(\{u_k\})$ exists. Moreover, when $\{x_k\} = \Psi(\{u_k\})$, $G_T : (x_{n-1}, x_n) \mapsto (x_n, x_{n+1})$ describes what we call the single-delay dynamics (SDD) in the space X . Thus using Γ , G_T can be realized as $G_T : (x_{n-1}, x_n) \mapsto (x_n, g(\Gamma(x_{n-1}, x_n), x_n))$, or in other words $G_T = (\pi_2, g) \circ (\Gamma, \pi_2)$ (see Fig. 1C in black-red), where π_2 is defined as $\pi_2 : (a, b) \mapsto b$ regardless on which product space the tuple (a, b) lies. In summary, learning $T = F'_S$ would enable us to forecast the time-series $\theta(\{w_n\})$, and regardless of S , and causal embedding property of g makes $\Gamma : Y_T \rightarrow U$ so that by the commutativity ladder in Fig. 1C, we have $T = \Gamma \circ (\pi_2, g) \circ (\pi_2, \Gamma) \circ H_2 \circ \varphi_T$. Note that $H_2 \circ \varphi_T$ is induced by g . Therefore, we can learn Γ in the “driven mode” of g where we make a sufficient collection of tuples (x_{n-1}, x_n) by feeding a finite segment of an orbit of T after the dynamics locks onto a solution due to UAP. Finally, we realize the iterates of G_T by: $G_T(x_{n-1}, x_n) = (x_n, g(\Gamma(x_{n-1}, x_n), x_n))$ and call the process of reading out $u_n = \Gamma(x_{n-1}, x_n)$ as an “autonomous run” of g .

Functional complexity of G_T . As the dimension of X i.e., N gets larger than the effective dimension of the input delay-coordinate vector $K \geq 2d + 1$ for a g in (1), empirical evidence suggests that the resultant map G_T turns “more linear” or has lower functional complexity as evidenced through the generalized Pearson correlation coefficients ([9]).

Global dissipativity (GD). We note that the embedding $f = H_2 \circ \varphi_T \circ P \circ \Phi_{2d,\theta}$ of W in $X \times X$ qualifies as a generalized synchronization in [22] where existential conditions are known for generic linear RNNs. Since causal embedding proves the existence of f , we can choose driven systems g that possess remarkable robustness to errors that linear systems do not possess. To clarify this, in the autonomous run of g , let us suppose that due to some small computational error, the map Γ we learn is not precise but has an error on a nonempty subset $E \subset Y_T$. Due to this learning error, $\Gamma(Y_T) \subset U^+$ where U^+ contains U . To handle a potentially enlarged input space U^+ in an autonomous run of g we can suppose to use a driven system $g^+ : U^+ \times X \rightarrow X$, an extension of $g : U \times X \rightarrow X$ that has the same state space X has the USP and is also SI-invertible. The RNN in (1) has this property due to the tanh function and due to SI-invertibility (see [9]). If h^+ denotes the universal semi-conjugacy of g^+ , its codomain X_U^+ contains X_U , the codomain of h since g^+ and g agree on $U \times X$. Thus for inputs from a dynamical system (U, T) , two successive solution values (x_{n-1}, x_n) of g^+ would be contained in $Y_T^+ \subset X_U^+ \times X_U^+$, and Y_T^+ contains Y_T . Thus the autonomous run of g^+ yields the iterates of $\tilde{G}_T = (\pi_2, g^+) \circ (\Gamma_{exp}, \pi_2)$, where $\Gamma_{exp} : Y_T^+ \rightarrow U^+$ and Γ_{exp} agrees with Γ on Y_T . Since the co-domain of \tilde{G}_T is still contained in the compact space $X \times X$ it can be shown that $X_{U^+} \times X_{U^+}$

contains an attractor of \tilde{G}_T (as indicated in Fig 1B) which of course contains Y_T^+ – we call this property of a driven system’s ability that permits stabilization of the noisy dynamics of (Y_T, G_T) towards an attracting set, global dissipativity (GD); see [9] for a formal treatment.

Importance of GD. We note that the GD notion here is different from the classical notion of structural stability – structural stability permits perturbations where a perturbed system is conjugate to the original system, and for forecasting, it is not enough to design read-outs from a system that is conjugate to the intended system. Instead, we wish for a “cushion” (here $X_{U^+} \times X_{U^+}$) around Y_T^+ that permits stabilization of trajectories towards the cushion in the event of an error. Indeed, during an autonomous run of g^+ , if the forecasting is erroneous for say j time-steps due to the non-emptiness of E , or more explicitly, the values $(\Gamma_{exp}(x_k, x_{k+1}), \dots, \Gamma_{exp}(x_{k+j}, x_{k+j+1}))$, are not close to being a segment of an orbit of T , even then the future dynamics of the autonomous run would not drift far away as it gets attracted into the set $X_{U^+} \times X_{U^+}$ (as indicated in Fig 1B). So, if suppose the tuples (x_{k+j+1}, x_{k+j+2}) returns to the set $Y_T - E$, the read-out in the autonomous run of g^+ would get stabilized back to the values of some orbit of T or in other words the iterates of \tilde{G}_T are precluded from veering off completely (see Fig. 1B). GD is later numerically illustrated (in Fig 1F and Fig 1G).

When Takens delay embedding does not hold. In such a case, we presume that the inputs to g are directly the elements of an orbit of an unknown dynamical system (V, F) ; here $V \subset \mathbb{R}^K$ and we do not assume the surjective map F to be necessarily continuous or invertible, and we set $P : V \rightarrow U$ to be the zero-padding map defined previously to obtain a system (U, T) whose orbits are vectors of length N (see Fig. 1D in yellow). The maps G_T and Γ exist whenever g is SI-invertible ([9] holds). The advantage of learning Γ rather than learning F from a typical orbit is that the SDD can be stabilized back as in Fig. 1B when g has global dissipativity. Even when T is not invertible, \hat{T} and G_T are conjugate, but the map $\varphi_T : U \rightarrow \hat{U}_T$ is not well-defined, and only $\vartheta_T : \hat{U}_T \rightarrow U$ given by $(\dots, u_{-2}, u_{-1}) \mapsto u_{-1}$ is well-defined. However, when g has SI-invertibility, a point (x_{n-1}, x_n) uniquely determines u_n , and thus a map $Y_T \rightarrow U$ indicated in green in Fig. 1D exists making (Y_T, G_T) a (dynamical) extension of (U, T) . So by learning G_T through Γ as before enables learning T .

Differences between the customary reservoir computing. In the conventional RC approach [31, 18] SI-invertibility of g is not guaranteed, and there is no evidence of a learnable function $x_j \mapsto u_j$ often calling for ad hoc adjustments like feedback connections [17] into the RNN. Here, we substantiate the well-defined SDD and learn the function Γ (using a deep learning technique) rather than simplifying the training procedure. We call the combined setup of an arbitrarily generated RNN, and a deep learning feedforward network a recurrent conjugate network (RCN) (see schematic

in [9]).

Numerical Experiments. We consider systems where the limiting behavior of a time-series $\{\theta(w_n)\}$ can be observed, a feature of systems where S is surjective. For example, the double pendulum (DP) system has a highly intricately woven invariant set owing to the fact that its dynamics is isomorphic to the product of a Bernoulli shift and a rotation of the circle [32]. The inherent effect of a rotation on the circle is that the auto-correlation of a trajectory could be aperiodic instead of vanishing rapidly with the lag, a feature of many chaotic systems considered in the literature. Building a model from data would require capturing the effect of the rotation and the chaotic dynamics of the Bernoulli shift. We describe the details of learning and training of Γ in [9] while an arbitrarily chosen observable θ (Fig. 1E) is considered for forecasting at discrete-time steps. In Fig. 1E, we present the multi-lag recurrence plot $(\theta(w(t)), \theta(w(t+8)), \theta(w(t+16)))$. To illustrate the advantage of global dissipativity, a zero-mean normally distributed noise vector is added to (x_{n-1}, x_n) , (i.e., to an orbit of G_T) every 100 time-steps in the autonomous mode to simulate Y_T^+ . The readouts when the system is driven (driven mode) in Fig. 1F are compared with such a noise-introduced autonomous run. Further, due to the high dimension of X , we plot three leading principal component analysis (PCA) values of (x_{n-1}, x_n) in Fig. 1G to illustrate how a trajectory in the autonomous mode (shown in blue) is stabilized back. Both these pictures illustrate the remarkable effect of GD which enable RCNs to forecast systems like the double pendulum that has not been achieved before.

By contrasting the outcomes of various popularly known methods, we further demonstrate the superiority of predicting using RCNs on other systems in [9]. In summary, we provided a Takens delay embedding’s stability challenge by learning a driven system’s single-delay dynamics. Employing a network in contrast to obtaining vector fields from data forfeits the interpretability of the learnt model, but the inscrutability of our approach comes with a prize of learning systems that have failed with existing methods due to either a lack of learnability or stability. A future study would identify conditions on the driven system for causal embedding to hold when an input $\{\theta(w_n)\}$ is fed sequentially rather than as delay coordinates, eliminating the requirement to know the length of the delay-coordinate vector. In [9], we present numerical findings by feeding $\{\theta(w_n)\}$ sequentially as well to address a real world problem.

References

- [1] Yule GU (1927) Vii. on a method of investigating periodicities disturbed series, with special reference to wolfer’s sunspot numbers. *Philosophical Transactions of the Royal Society of London. Series A, Containing Papers of a Mathematical or Physical Character* 226(636-646):267–298.

- [2] Takens F (1981) Detecting strange attractors in turbulence in *Dynamical systems and turbulence, Warwick 1980*. (Springer), pp. 366–381.
- [3] Sauer T, Yorke JA, Casdagli M (1991) Embedology. *Journal of statistical physics* 65(3):579–616.
- [4] Stark J (1999) Delay embeddings for forced systems. i. deterministic forcing. *Journal of Nonlinear Science* 9(3):255–332.
- [5] Gutman Y, Qiao Y, Szabó G (2018) The embedding problem in topological dynamics and takens theorem. *Nonlinearity* 31(2):597.
- [6] De Vries J (2013) *Elements of topological dynamics*. (Springer Science & Business Media) Vol. 257.
- [7] Casdagli M, Eubank S, Farmer JD, Gibson J (1991) State space reconstruction in the presence of noise. *Physica D: Nonlinear Phenomena* 51(1-3):52–98.
- [8] Munkres J (2014) *Topology*. (Pearson Education).
- [9] Manjunath G, Clercq A, Steynberg M (2022). *Supporting Information that is available online along with this publication*.
- [10] Bakker R, Schouten JC, Giles CL, Takens F, Van Den Bleek CM (2000) Learning chaotic attractors by neural networks. *Neural Computation* 12(10):2355–2383.
- [11] Principe JC, Rathie A, Kuo JM (1992) Prediction of chaotic time series with neural networks and the issue of dynamic modeling. *International Journal of Bifurcation and Chaos* 2(04):989–996.
- [12] Schmid PJ (2010) Dynamic mode decomposition of numerical and experimental data. *Journal of fluid mechanics* 656:5–28.
- [13] Williams MO, Kevrekidis IG, Rowley CW (2015) A data-driven approximation of the koopman operator: Extending dynamic mode decomposition. *Journal of Nonlinear Science* 25(6):1307–1346.
- [14] Xu D, Lu F (2006) Modeling global vector fields of chaotic systems from noisy time series with the aid of structure-selection techniques. *Chaos: An Interdisciplinary Journal of Nonlinear Science* 16(4):043109.
- [15] Brunton SL, Proctor JL, Kutz JN (2016) Discovering governing equations from data by sparse identification of nonlinear dynamical systems. *Proceedings of the national academy of sciences* 113(15):3932–3937.
- [16] Champion K, Lusch B, Kutz JN, Brunton SL (2019) Data-driven discovery of coordinates and governing equations. *Proceedings of the National Academy of Sciences* 116(45):22445–22451.
- [17] Jaeger H, Haas H (2004) Harnessing nonlinearity: Predicting chaotic systems and saving energy in wireless communication. *Science* 304(5667):78–80.

- [18] Lu Z, Hunt BR, Ott E (2018) Attractor reconstruction by machine learning. *Chaos: An Interdisciplinary Journal of Nonlinear Science* 28(6):061104.
- [19] Herteux J, R ath C (2020) Breaking symmetries of the reservoir equations in echo state networks. *Chaos: An Interdisciplinary Journal of Nonlinear Science* 30(12):123142.
- [20] Manjunath G (2021) An echo state network imparts a curve fitting. *IEEE Transaction on Neural Networks and Learning Systems*; doi: 10.1109/TNNLS.2021.3099091.
- [21] Faranda D, et al. (2019) Boosting performance in machine learning of turbulent and geophysical flows via scale separation.
- [22] Grigoryeva L, Hart A, Ortega JP (2021) Learning strange attractors with reservoir systems. *arXiv preprint arXiv:2108.05024*.
- [23] Manjunath G, Jaeger H (2013) Echo state property linked to an input: Exploring a fundamental characteristic of recurrent neural networks. *Neural computation* 25(3):671–696.
- [24] Maass W, Natschl ager T, Markram H (2002) Real-time computing without stable states: A new framework for neural computation based on perturbations. *Neural computation* 14(11):2531–2560.
- [25] Grigoryeva L, Ortega JP (2018) Echo state networks are universal. *Neural Networks* 108:495–508.
- [26] Manjunath G (2020) Stability and memory-loss go hand-in-hand: three results in dynamics and computation. *Proceedings of the Royal Society A* 476(2242):20200563.
- [27] Manjunath G (2022) Embedding information onto a dynamical system. *Nonlinearity* 35(3):1131.
- [28] Ingram WT, Mahavier WS (2011) *Inverse limits: From continua to Chaos*. (Springer Science & Business Media) Vol. 25.
- [29] Grigoryeva L, Hart A, Ortega JP (2021) Chaos on compact manifolds: Differentiable synchronizations beyond the takens theorem. *Physical Review E* 103(6):062204.
- [30] Manjunath G, Jaeger H (2013) Echo state property linked to an input: Exploring a fundamental characteristic of recurrent neural networks. *Neural computation* 25(3):671–696.
- [31] Jaeger H (2001) The echo state approach to analysing and training recurrent neural networks-with an erratum note. *Bonn, Germany: German National Research Center for Information Technology GMD Technical Report* 148(34):13.
- [32] Ornstein DS (1989) Ergodic theory, randomness, and “chaos”. *Science* 243(4888):182–187.

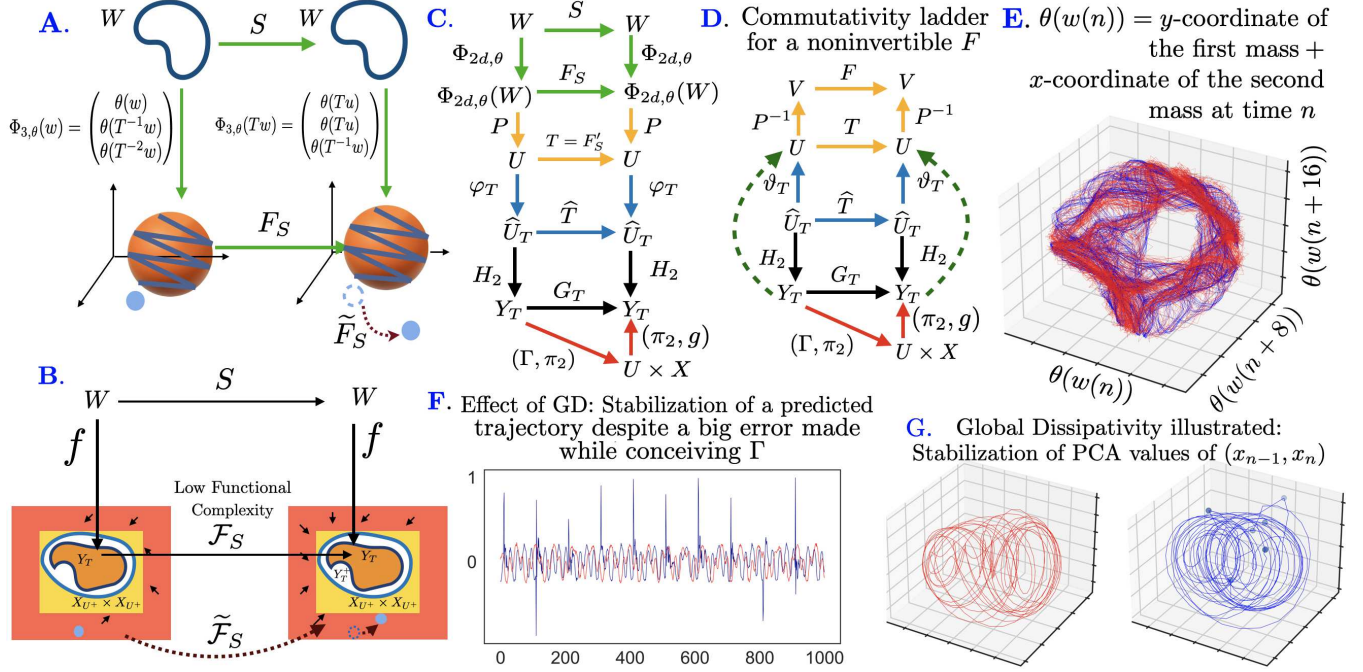


Figure 1: **A.** Schematic of employing the Takens embedding and the effect of iterates of \tilde{F}_S slipping out of $\Phi_{\theta,2d}(W)$. **B.** Schematic to illustrate the effect of global dissipativity. **C.** Commutativity ladder: inner workings of a conjugate system when the Takens theorem holds. **D.** Commutativity ladder with input being an orbit from a non-invertible system. **E.** Multi-lag recurrence plot of a forecasted time-series from an observation θ of a Double Pendulum System with a zero-mean normally distributed noise with standard deviation 0.01; the points $(\theta(w(t)), \theta(w(t+8)), \theta(w(t+16)))$ of the actual (in red) and forecasted (in blue) values are plotted. In this experiment the RNN matrices A and B in Eqn. (1) were initialized randomly, with B having a unit spectral radius and the delay-coordinates always padded with the needed amount of zeroes to match A 's row number; also $X = [-1, 1]^{1000}$, $a = 0.5$ and $\alpha = 0.99$. After discarding 1000 tuples (x_{n-1}, x_n) to forget its original state, Γ is learnt using 5000 such tuples. **F.** Effect of GD: The underlying tuples (x_{n-1}, x_n) of the data in (E) is perturbed by a high-amplitude Gaussian noise vector with standard deviation 2 once in every 100 time-steps in the autonomous mode of g to simulate an error in Γ ; despite this the readout in (blue) stabilizes towards the pattern of the actual readout conceived in the driven mode (red). **G.** Illustration of GD: three largest principal component analysis (PCA) values of (x_{n-1}, x_n) corresponding to the time-series shown in F is plotted for the driven (red) and autonomous (blue) mode; successive points are joined; thick dots show the high-amplitude noise instants. The blue trajectory drifts but is stabilized back.

This figure "Fig_Big.png" is available in "png" format from:

<http://arxiv.org/ps/2105.10759v3>